Waste and Biomass Valorization (2021) 12:2357–2364
https://doi.org/10.1007/s12649-020-01146-7

ORIGINAL PAPER

Deoxygenation of Methyl Oleate and Commercial Biodiesel Over W and Ni-W Catalysts

Gagandeep Singh Dhillon[1] · **Palligarnai T. Vasudevan**[1]

Received: 13 January 2020 / Accepted: 29 June 2020 / Published online: 16 July 2020

Abstract

The enhancement of biodiesel fuel properties by modifying/optimizing fatty ester composition is an area of ongoing research. Chemical upgrading methods include catalytic hydrodeoxygenation process (HDO), hydrothermal liquefaction, Fischer–Tropsch synthesis (F–T synthesis), and super-critical modification. Catalytic hydrodeoxygenation process for converting biodiesel into renewable petrodiesel-like fuels substitutes is gaining considerable importance. The biodiesel upon hydrotreatment produces green diesel that has a cetane number higher than commercial petroleum diesel. In this paper, we report the findings of using tungsten as a deoxygenation catalyst supported over γ–Al_2O_3 to convert methyl oleate and biodiesel to green diesel. The catalysts were characterized by XPS analysis and N_2 adsorption–desorption. The effect of reduction temperature, hydrogen flowrate, Ni promoter and anion (oxide vs sulfide catalyst) on the hydrodeoxygenation activity of the catalyst were examined. It was found that catalyst reduced at 300/350 °C was optimal from a selectivity point of view. Moreover, increasing the hydrogen flowrate favored hydrodeoxygenation over decarbonylation/decarboxylation. It was further deduced that Ni promoted the activity and that the oxide catalyst was superior in this respect to the sulfide catalyst.

Graphic Abstract

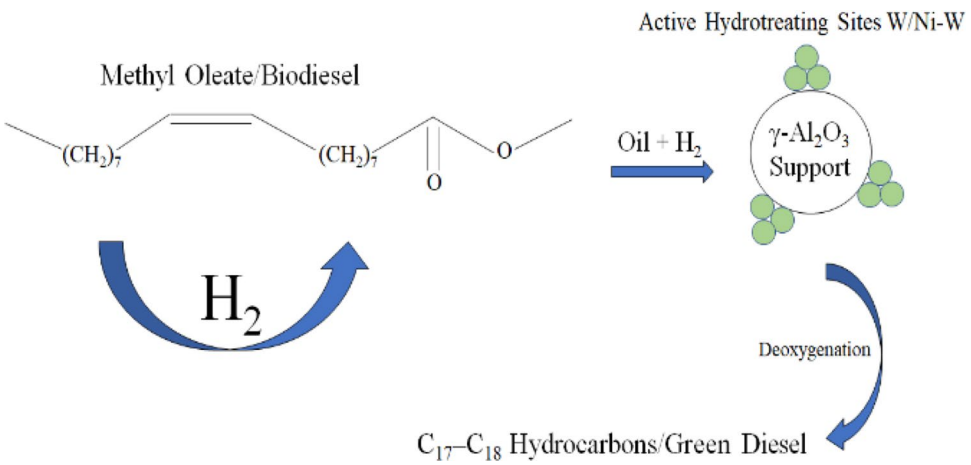

Keywords Methyl oleate · Biodiesel · W catalyst · Ni promoter · Hydrodeoxygenation

Statement of Novelty

The main objective of this research was to explore hydrotreating tungsten catalysts for the production of green diesel from biodiesel. Hydrotreating catalysts such as Mo, Ni, Co, etc. have been investigated in the past, but not many

Electronic supplementary material The online version of this article (https://doi.org/10.1007/s12649-020-01146-7) contains supplementary material, which is available to authorized users.

✉ Palligarnai T. Vasudevan
vasu@unh.edu

[1] Department of Chemical Engineering, University of New Hampshire, Durham, NH 03824, USA

reports are available on W–based catalysts. In this study, it was found that W–catalysts had pronounced activity for deoxygenation of methyl oleate and commercial biodiesel. More importantly, the conversion of methyl oleate reached almost 100% by promoting W with Ni. Earlier studies on deoxygenation of oleic acid and methyl oleate over precious metals such as Pt also showed promising results. However, employment of precious metals in industry might prove uneconomical. Thus, inexpensive catalysts such as W and/or Ni-W might prove cost-effective while simultaneously giving high activities.

Introduction

Methods employed to remove heteroatoms such as S, N and O as H_2S, NH_3 and H_2O in petroleum feedstocks are commonly known as hydrodesulfurization (HDS), hydrodenitrogenation (HDN) and hydrodeoxygenation (HDO), respectively [1]. Biodiesel comprises of long chain esters of fatty acid—also known as Fatty Acid Methyl Ester (FAME) and it can be produced by transesterification of triglyceride feedstock. Hydrodeoxygenation of FAME gives a hydrocarbon in the range C_{15}–C_{18} known as green diesel, which has high cetane number [2]. Biodiesel can be synthesized from triglycerides-based feedstock such as sunflower oil, coconut oil, jatropha oil, palm oil and rapeseed oil [3]. The main pathway in the formation of green diesel (C_{15}–C_{18}) from FAME involves decarbonylation or/and decarboxylation, which proceeds by hydrogenation of unsaturated C=C bonds, progressive hydrogenolysis of the C=O bond to fatty acid and finally reduction to hydrocarbons. The second route in hydrocarbon formation, known as hydrodeoxygenation, involves the above-mentioned steps leading to the formation of intermediate alcohols by dehydration on acid sites of support and then hydrogenation on active metal sites to produce hydrocarbons [3–5]. In hydrotreating reactions, γ-alumina is generally used as support due to its high surface area (~ 200 m^2/g). But it suffers from coking due to its strong interaction with the metal species and to overcome this drawback, carbon is used as support due to its amphoteric properties and surface inertness [6]. The commonly used hydrodeoxygenation catalysts are supported noble and sulfide or oxide metal catalysts such as Co–Mo/Al_2O_3, Ni–Mo/Al_2O_3 and W–Ni/Al_2O_3 [7]. W-based catalysts have been reported to have better properties than Mo-based catalysts [8]. Organometallic catalysts of Ni and Mo are reported to be highly reactive and reaction specific—thereby minimizing side reactions [9]. Transition metal phosphides of Ni, W, Mo and Fe have been proven highly active for HDS and HDN of petroleum feedstocks. Of all the aforementioned catalysts for hydrotreating reactions, Ni_2P prepared by phosphate precursor is the most effective catalyst [10]. 5 wt% Ni/Al_2O_3 has been studied for HDO of stearic acid and tall oil fatty acids at reaction temperature of 300 °C and it was found that overall conversion for unreduced catalyst was 31%, and for reduced catalysts, 99%. This necessitates the requirement of catalyst reduction [11]. Sulfur free Ni catalysts have been studied for production of green diesel by HDO over Ni catalyst and it was found that transformation of stearic acid was more rapid over Ni/HY than over Ni/Al_2O_3 and Ni/SiO_2, giving respective conversions values after 90 min of 94%, 43%, and 46% [2]. Ni-alumina co-precipitated catalysts give complete conversion of sunflower oil into hydrocarbons in the diesel range and the heating value of this product was calculated to be almost equal to 43.9 MJ/kg, which is very close to the heating value of diesel (43.4 MJ/kg) [5]. Ni and Mo oxalates are found to be effective in producing more iso-paraffins along with normal paraffins [12]. Ni–Mo catalysts have been extensively studied for hydrodeoxygenation reactions and it is found that CO and CO_2 are formed as by-product gases which are readily converted to CH_4 due to high activity of Ni towards methane formation in the presence of hydrogen, and the reaction follows first order kinetics [13, 14]. Ni–Mo catalysts with similar Ni/(Ni + Mo) ratios revealed that sulfide catalysts have better activity compared to the reduced oxide catalysts [15]. In the case of noble metals catalysts like Pd, Pt and Rh, the reaction proceeds through decarbonylation and decarboxylation [4, 16–18], whereas for Fe based catalysts, the formation of hydrocarbons is supposed to proceed via HDO [19]. Transitional metal phosphides of Ni, Co and W have proven to be active in deoxygenation of biofuel compounds and the reaction proceeds via decarbonylation [10]. Hydroprocessing of waste soya oil, jatropha oil and C_{18} fatty acids has been studied over sulfide Ni–W/SiO_2–Al_2O_3 catalyst and it is found that this catalyst favors decarbonylation and decarboxylation, producing kerosene range products along with diesel range products [20–23]. W_2C supported on carbon nanofibers produced olefins in the hydrodeoxygenation of oleic acid [24].

In this study, we used tungsten oxide (WO_3) and sulfide (WS_2) catalysts along-with Ni-promoted tungsten catalysts supported on γ–Al_2O_3 for deoxygenation of methyl oleate and commercial biodiesel to produce green diesel. To the best of our knowledge, inexpensive W/Ni-W oxide and sulfide catalysts have not been investigated for deoxygenation of methyl oleate and commercial biodiesel under conditions used in this study. In this research, effect of reduction temperature, H_2 flowrate, effect of Ni promoter and comparison between oxide and sulfide catalysts is studied. Unpromoted WO_3 catalysts showed ~ 98% conversion of methyl oleate after 4 h (time on-stream) TOS. Addition of Ni facilitated nearly 100% conversion. Earlier studies on deoxygenation of triglycerides such as sunflower oil and rapeseed oil over Ni–W/Al_2O_3 catalysts demonstrated ~ 95% conversion at 380 °C and 20 bar pressure

[25]. Supported tungsten oxide catalysts find numerous applications in hydrodesulfurization, hydrodenitrogenation, hydrodeoxygenation, hydrocarbon cracking, olefin metathesis alkane isomerization and selective catalytic reduction [26].

Experimental

Catalyst Preparation

All the catalysts were prepared by wet impregnation as described elsewhere [27–31]. 15 g of ammonium meta-tungstate were dissolved in 50 mL water and 15 mL ammonium hydroxide solution to form a uniform saturated solution. Impregnation was carried out at room temperature by introducing 25 g of γ-alumina (average pore size 125 Å, diameter 3.5 mm) to this saturated solution and blanketed under nitrogen gas at room temperature (25 °C) for 24 h. The equilibrated γ-alumina was separated by filtration and then calcined in an oven at 400 °C for 2 h. This calcining procedure thermally decomposed the ammonium meta-tungstate into immobilized WO_3 on γ-Al_2O_3. For Ni promoted WO_3, 5 g of $Ni(NO_3)_2$ $6H_2O$ was dissolved in 40 mL water to form a homogeneous solution and then 15 g of as-synthesized WO_3/γ-Al_2O_3 was added to it. The mixture was then left for 48 h and then calcined at 400 °C for 2 h to get $NiWO_x$. For sulfide catalysts, ammonium tetrathiotungstate was used as the W precursor and a similar procedure was employed to synthesize the catalyst except that the catalyst was separated under vacuum filtration and then dried in a vacuum desiccator. Supported catalysts were then thermally decomposed in the reactor with H_2 to give WS_2 or $NiWS_x$.

Catalyst Characterization

N_2 adsorption–desorption isotherms were carried out using NOVA 2200 s Surface Area and Pore Size Analyzer. The Brunauer–Emmett–Teller (BET) method was used to estimate the surface area of the catalyst samples and pore radius was determined using Barret–Joyner–Halenda (BJH) method and the pore volume was obtained from t-plot. X-ray Photoelectron Spectroscopy (XPS) was performed under high vacuum conditions (P~10^{-8} millibar) using Kratos Axis HS equipped with dual achromatic gun with Al and Mg sources. XPS spectra were obtained by irradiating the sample with a beam of monoenergetic Mg Kα X-rays (1253.6 eV) while simultaneously measuring the kinetic energy and number of electrons that escape from the top 0 to 10 nm of the material being analyzed. The binding energy was obtained by referencing to the C 1 s line taken as 284.8 eV.

Reaction Setup

Typically, the catalytic HDO process contained three steps: (i), pretreatment of the catalyst by hydrogen gas (ii), reaction step with biodiesel and hydrogen gas, with samples periodically analyzed by gas chromatography (GC); and (iii), cleaning and drying step of catalyst by inert gas. Based on these steps, an auto-sampling bubbler-reactor system was designed and assembled. The system essentially consisted of a stainless-steel microreactor (6.35 × 107.95 mm) and a stainless-steel bubbler (31.75 × 107.95 mm.) equipped with three 3-way valves that permitted in situ pretreatment, reaction, and activity measurement of the catalyst. The lines between the bubbler, the microreactor, and the line downstream of the reactor were stainless-steel coil (6.35 mm) wrapped with heating tape to prevent condensation of reactants. There also were heating lamps around the whole system to provide a constant temperature environment. All the sample points were covered with silica septa and the samples were taken by a gas-proof pressure-lock syringe and analyzed by gas chromatography (Hewlett Packard 5890). For catalytic activity studies, the reactor was loaded with 0.1 g of catalyst as well as glass wool, and the bubbler was loaded with 120 mL biodiesel or methyl oleate and 12 mL iso-octane solvent. The reaction was carried out at 400 °C and 289,579 Pa hydrogen pressure. Prior to the reaction, the catalyst was reduced under pure hydrogen at 300˚C and hydrogen flowrate was 60 mL/min. In the analysis step, helium gas was used as a carrier for the GC and the flow rate was set at 2.52 mL/min. Hydrogen and compressed air were used for the FID, and the flow rates were set at 30.8 mL/min and 300 mL/min, respectively. The injector temperature of GC was kept at 180 °C and the detector temperature at 350 °C. The initial temperature of the GC oven was set at 180 °C, and this temperature was kept for 2 min. Then the oven temperature was increased to 220 °C at a rate of 10 °C/min. The final temperature of 220 °C was kept for 30 min. The data were transferred to a computer with the help of Peak96 software. The data files were analyzed by Origin-8 software to calculate the areas of all peaks. Conversion of methyl oleate/biodiesel (Fatty Acid Methyl Ester) and C_{18}/C_{17} ratio of green diesel were calculated according to the following equations.

$$\%Conversion = \left(\frac{FAME_{in}(g) - FAME_{out}(g)}{FAME_{in}(g)} \right) * 100$$

$$\frac{C_{18}}{C_{17}} = \frac{Octadecane_{out}(g)}{Heptadecane_{out}(g)}$$

where, $FAME_{in}$ (g) and $FAME_{out}$ (g) are the amounts of Fatty Acid Methyl Ester fed in inlet and outlet stream

respectively. Similarly, octadecane $_{out}$ (g) and heptadecane $_{out}$ (g) represents their respective amounts formed during deoxygenation reaction.

Results and Discussion

Catalyst Characterization

Figure 1a, b shows the sorption isotherms of W and Ni promoted W oxide and sulfide catalysts. All the samples exhibit type IV isotherm, which resembles the mesoporous solids having pore size distribution in the range of 20–500 Å. As shown in the Table 1, the pore radius of all the samples fall

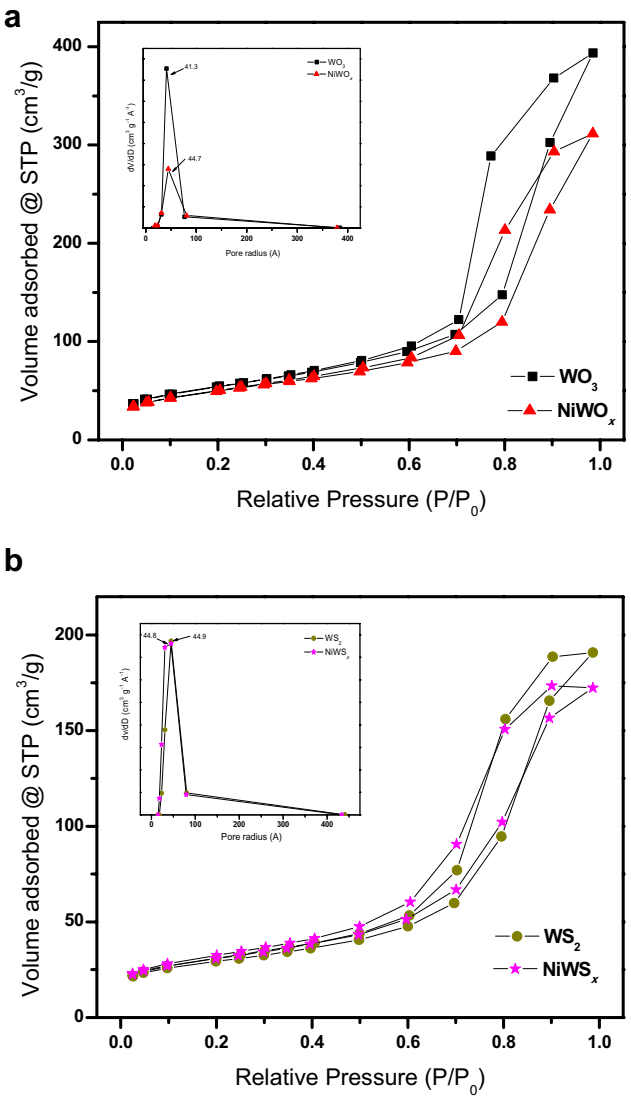

Fig. 1 **a** N_2 adsorption—desorption isotherms of WO_3 and $NiWO_x$ catalysts supported over γ-Al_2O_3. **b** N_2 adsorption—desorption isotherms of WS_2 and $NiWS_x$ catalysts upported over γ-Al_2O_3

Table 1 Textural properties of tungsten and nickel promoted tungsten oxide and sulfide catalysts

	WO_3	$NiWO_x$	WS_2	$NiWS_x$
Surface Area (m^2/g)	191	176	100	106
Pore volume (cm^3/g)	0.64	0.48	0.31	0.28
Pore radius (Å)	41.3	44.7	44.9	44.8
Metal loading (wt%)	7% W	5% W 1.5% Ni	14% W	24.5% W 5% Ni

in the above range indicating the formation of mesoporous catalysts. The pore volume decreased for both the oxide and sulfide catalyst upon addition of Ni promoter from 0.64 to 0.48 cm^3/g and 0.31 to 0.28 cm^3/g respectively. The pore radius of WS_2 and Ni promoted WS_2 does not change significantly but it changes for WO_3 and Ni promoted WO_3 from 41.3 to 44.7 Å; this increase can be attributed to insertion of Ni/W into the lattice of γ-Al_2O_3 support [32]. The BET surface area of WO_3 catalyst decreases upon Ni addition from 191 to 176 m^2/g but increased for WS_2 upon Ni insertion from 100 to 106 m^2/g.

XPS analysis of the oxide catalysts are presented in Fig. 2a. It shows that tungsten is present as WO_3 in the form of + 6 oxidation state. The peak at 35.7 eV can be ascribed to W $4f_{7/2}$ spin-orbital split and peak at 37.9 eV can be attributed to W $4f_{5/2}$ spin-orbital split. Similar observations are seen in the literature for W 4f spectrum [24, 32]. Also, there is a third peak at 36.7 eV which could be attributed to presence of aluminum tungstate species and this is suggested to be formed by the interaction between surface tungsten oxide species and γ-Al_2O_3 support during calcination [33]. For NiO promoted WO_3 catalyst, W $4f_{7/2}$ peak shifts to higher binding energy at 36.2 eV and W $4f_{5/2}$ peak shifts to 38.5 eV. This shift in the binding energy to higher values suggests that Ni-W interactive species might be present on the surface of catalyst. Additionally, the binding energy values of W^{6+} in W and Ni-W oxide catalysts reported here are approximately 1 eV higher compared to the one reported in literature [33]. This discrepancy in binding energy values could be attributed to differences in the referencing element employed for calibration. Ng. et al. [33] employed Au $4f_{7/2}$ line at 83.8 eV for calibration of XPS spectra, while we employed C 1 s line taken as 284.8 eV for calibration. A similar idea for discrepancies in binding energy values was also suggested by Ng. et al. [33]. Figure 2b shows the XPS analysis of tungsten sulfide and Ni promoted tungsten sulfide catalyst. W 4f spectra of unpromoted sulfide catalyst show two peaks at 33.4 eV and 35.9 eV and these peaks are due to $4f_{7/2}$ and $4f_{5/2}$ spin-orbital split respectively [32]. It revealed that tungsten is present as WS_2 with + 4 oxidation state. However, Ni promoted WS_2 showed two distinct peaks around 35.5 eV and 37.3 eV which corresponds to + 6

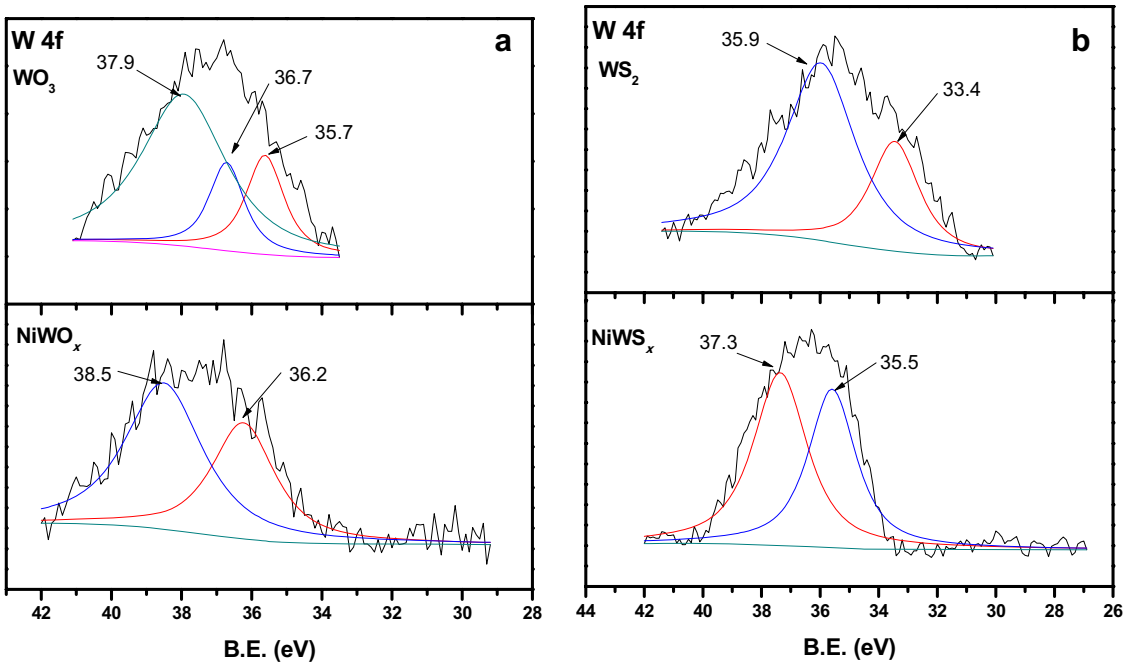

Fig. 2 **a** W 4f spectra in WO_3 and $NiWO_x$ supported over γ-Al_2O_3. **b**.W 4f spectra in WS_2 and $NiWS_x$ supported over γ-Al_2O_3

oxidation state of W. This suggests that W^{4+} in WS_2 might have been oxidized to W^{6+} during impregnation with nickel nitrate which decomposes to NiO upon calcination.

Effect of Pretreatment Temperature

Pretreatment is an important step to promote and maintain the activity of the catalyst. In the catalytic HDO process, pretreatment of the catalyst by hydrogen at a certain temperature reduces the metal oxide and provides the active sites used in further reaction steps. This reduction procedure is mainly affected by temperature; thus, study of the pretreatment temperature is an important and necessary step. It has been demonstrated that WO_3 supported on γ-Al_2O_3 upon reduction in hydrogen still remains in + 6 oxidation state even if reduced at temperatures as high as 500 °C [33]. As shown in the Fig. 3, when increasing the pretreatment temperature from 250 to 400 °C, the overall conversion increases from 82 to 98%. There could be two plausible reasons for increased conversion of methyl oleate with increase in reduction temperature. (1) During reduction, dissociation of H_2 on WO_3 sites might facilitate its spill-over on catalyst surface. Such phenomenon might assist the formation of W–OH species, which are supposed to be responsible for fatty acid activation [32]. So, increase in reduction temperature might increase the formation of active W–OH species. (2) It has been shown in literature that WO_3 forms aluminum tungstate ($Al_2(WO_4)_3$) complex during calcination procedure [33]. However, aluminum tungstate is less stable than

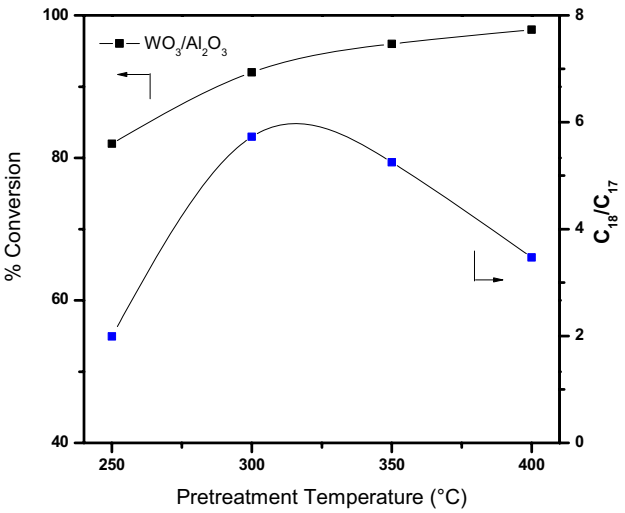

Fig. 3 Effect of pretreatment temperature on overall conversion of methyl oleate

W^{6+} species at higher reduction temperature [33]. Thus, increasing the reduction temperature from 250 to 400 °C might decrease the concentration of tungstate complex and simultaneously form active W^{6+} species. Maximum C_{18}/C_{17} ratio of ~ 5.8 is observed at a reduction temperature of 300 °C. However, increasing the reduction temperature to 350 or 400 °C, decreases the C_{18}/C_{17} ratio. Such behavior suggests dominance of decarbonylation/decarboxylation at higher reduction temperatures. Moreover, at 250 °C

reduction temperature, formation of lower hydrocarbons in the kerosene range is evident from Fig. S1. This could be attributed to the formation of $Al_2(WO_4)_3$ interaction complex, which might be responsible for cracking of hydrocarbon chain due to its acidic property. And upon increasing the reduction temperature to 400 °C, there are no peaks of lower hydrocarbons as shown in Fig. S2 to Fig. S4 suggesting the absence of aluminum tungstate complex at this reduction temperature.

Effect of Hydrogen Flowrate

Hydrogen flowrate plays a key role in the hydrodeoxygenation process, especially in overall biodiesel conversion and deoxygenation pathway selection. Additionally, hydrogen gas also acts as a carrier gas for biodiesel in the experimental system. In this study, three hydrogen flow rates (40, 60 and 80 mL/min) were investigated with the WO_3/γ-Al_2O_3 catalyst. The results are shown in Fig. 4. It is clear that on increasing the hydrogen flowrate from 40 to 80 mL/min, the overall methyl oleate conversion increases from 89 to 99%. One plausible explanation for this is that external mass transport can be enhanced by a better mixing of the fluid. A higher flowrate of hydrogen contributes to enhanced mass transfer by reducing the laminar film around the catalyst particle and ensuring that more reactants are transported to the surface of catalyst. At low hydrogen flowrates, it is also conceivable that there is more adsorption of methyl oleate or biodiesel on the catalyst leading to reduction in surface area. The C_{18}/C_{17} ratio increases from three to six as hydrogen flowrate increases from 40 to 80 mL/min. Probably, there are two reasons for this: (1) hydrogen is also a carrier gas; higher hydrogen flow rate can produce a higher bulk flow rate that benefits the mass-transfer rate, and (2) the mass of methyl oleate per volume of input gas decreases, which results in a higher hydrogen/oil ratio. This benefits the hydrodeoxygenation reaction.

Effect of Promoter

Figure 5 shows TOS dependence of methyl oleate and commercial biodiesel conversion over W and Ni-W catalysts. It can be observed that conversion of methyl oleate over WO_3/γ-Al_2O_3 catalyst increases from 72 to 94% from 1 to 4 h TOS respectively. The increase in methyl oleate conversion with TOS could be due a lower partial pressure of H_2 before it reaches steady state. Similar observations of increased conversion of oil with TOS has been previously reported in literature [24, 32]. However, for deoxygenation of commercial biodiesel, it is found that its conversion is lower than methyl oleate. This behavior might be ascribed to the presence of saturated fatty acid esters in commercial biodiesel that show relatively less reactivity than unsaturated fatty acid esters. Specifically, presence of double bond in hydrocarbon chain cause the molecule to 'bend'. Due to this, the intermolecular attraction force decreases. On the other hand, the geometry of hydrocarbon chain in saturated fatty acid ester is relatively linear. This causes the molecules to compact tightly thereby increasing the intermolecular attraction forces. Effect of Ni promoter on deoxygenation of methyl oleate and commercial biodiesel suggests that addition of Ni enhanced the catalytic activity. For instance, the overall conversion of methyl oleate increased from 93 to 100% while that of commercial biodiesel increased from

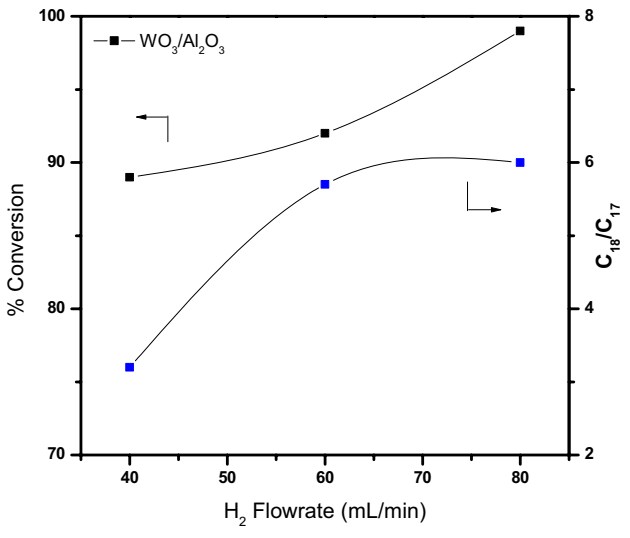

Fig. 4 Effect of hydrogen flowrate on overall conversion of methyl oleate

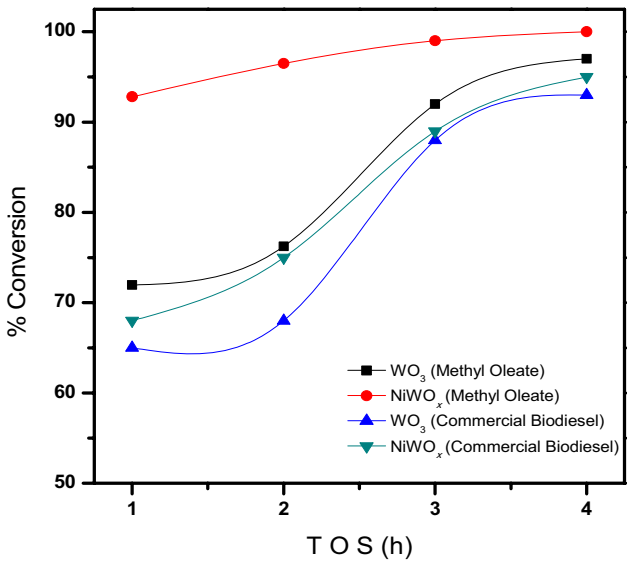

Fig. 5 Effect of Ni promoter on the catalytic activity

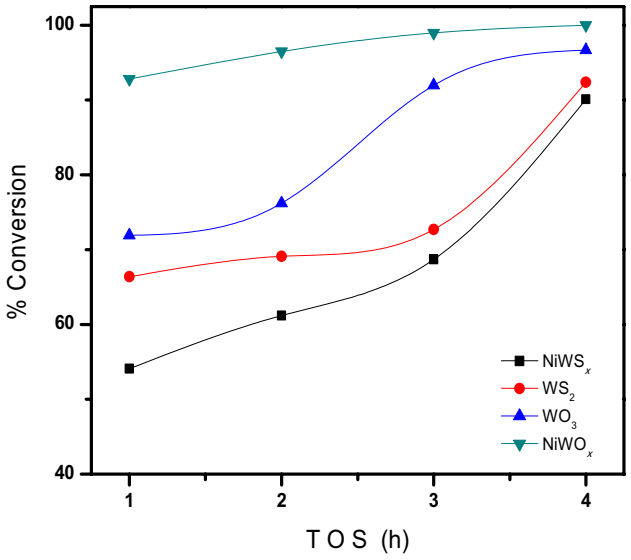

Fig. 6 Comparison between oxide and sulfide catalysts on HDO activity of methyl oleate

68 to 93% with TOS. This could be attributed to the presence of two hydrotreating sites, viz. Ni and W which might increase the catalytic activity. Deoxygenation of natural triglycerides such as sunflower oil and rapeseed oil also facilitated ~ 95% conversion over Ni-W/Al_2O_3 catalyst at 380 °C and 20 bar pressure [25]. Moreover, Pt-WO_x/Al_2O_3 has been proven to be better than individual monometallic catalysts for deoxygenation of methyl oleate and oleic acid [32]. Ni-W supported on TiO_2 for hydrodeoxygenation of guaiacol also showed excellent catalytic activity giving 100% conversion with cyclohexane and benzene as main products formed through decarboxylation route [34]. Thus, addition of Ni promoter to WO_3 catalyst is reasonable for deoxygenation of oil to diesel range hydrocarbons.

Comparison Between Oxide and Sulfide Catalysts

Figure 6 reveals that overall conversion for oxide catalyst is higher compared to sulfide catalyst. The conversion of methyl oleate over WS_2 increases from 66 to 92% whereas the conversion of methyl oleate over $NiWS_x$ catalyst increases from 54 to 90%. The low conversion of WS_2 compared to WO_3 could be attributed to low BET surface area of WS_2 as shown in Table 1. Hence, it is envisaged that an optimum metal loading is essential to obtain high catalytic activity. Low conversion of $NiWS_x$ compared to $NiWO_x$ catalyst could be due to two reasons: (1) It has been shown in literature that upon sulfidation of Ni–W catalysts, Ni–W–S active phase is formed [34]. This active phase might generate co-ordinate unsaturation sites (CUS) upon reduction which are supposed to be catalytically active sites in hydrotreating reactions [33]. However, XPS analysis showed formation of nickel oxide (peak at 854.7 eV, not shown here) instead of nickel sulfide because nickel nitrate was used as precursor for synthesizing Ni promoted WS_2 catalyst. Employment of nickel nitrate as Ni precursor would form NiO upon calcination. Thus, active Ni–W–S phase might not have been formed in $NiWS_x$ thereby inhibiting the catalytic activity. Sulfide catalyst could be also prepared by sulfiding under H_2S/H_2 atmosphere at elevated temperatures but strong interaction of NiO and WO_3 with the support hinders its application [35]. (2) Low BET surface area of $NiWS_x$ compared to $NiWO_x$ catalyst might explain its low conversion.

Conclusions

In this research, hydrotreating tungsten and nickel promoted tungsten catalyst was used to study the hydrodeoxygenation reaction for production of green diesel from methyl oleate/biodiesel. Effects of pretreatment (reduction) temperature, hydrogen flowrate, promoter and anion (oxide vs sulfide) were investigated. Pretreatment temperature is the most important parameter for green diesel selectivity. It is found that at low reduction temperature (250 °C), hydrodeoxygenation is also favored along with decarbonylation and decarboxylation. At higher reduction temperatures (300 °C and 350 °C) more selectivity towards green diesel is achieved indicating only two reaction pathways i.e. decarbonylation and decarboxylation. It is concluded that pretreatment temperature of 300–350 °C is ideal for carrying out deoxygenation reaction with W catalyst. Increasing the hydrogen flowrate from 40 to 80 mL/min leads hydrodeoxygenation over decarbonylation and decarboxylation. Addition of Ni increases the activity and also prevents the formation of lower hydrocarbons (C_{10}–C_{15}). It is found that overall conversion with oxide catalyst is higher than sulfide catalyst.

Compliance with Ethical Standards

Conflict of interest The authors declare that they have no conflict of interest.

References

1. Furimsky, E.: Catalytic hydrodeoxygenation. Appl. Catal. A Gen. **199**, 147–190 (2000)
2. Hachemi, I., Kumar, N., Arvela, P.M., Roine, J., Peurla, M., Hemming, J., Salonen, J., Murzin, D.Y.: Sulfur-free Ni catalyst for production of green diesel by hydrodeoxygenation. J. Catal. **347**, 205–221 (2017)
3. Kordulis, C., Bourikas, K., Gousi, M., Kordouli, E., Lycourghiotis, A.: Development of nickel based catalysts for the transformation of natural triglycerides and related compounds into green diesel: a critical review. Appl. Catal. B. **181**, 156–196 (2016)

4. Bie, Y., Lehtonen, J., Kanervo, J.: Hydrodeoxygenation (HDO) of methyl palmitate over bifunctional Rh/ZrO_2 catalyst: Insights into reaction mechanism via kinetic modeling. Appl. Catal. A Gen. **526**, 183–190 (2016)
5. Gousi, M., Andriopouloua, C., Bourikasb, K., Ladasc, S., Sotirioub, M., Kordulisa, C., Lycourghiotisa, A.: Green diesel production over nickel-alumina co-precipitated catalysts. Appl. Catal. A Gen. **536**, 45–56 (2017)
6. Varakin, A.N., Salnikov, V.A., Nikulshina, M.S., Maslakov, K.I., Mozhaev, A.V., Nikulshin, P.A.: Beneficial role of carbon in Co(Ni)MoS catalysts supported on carbon-coated alumina for co-hydrotreating of sunflower oil with straight-run gas oil. Catal. Today **292**, 110–120 (2017)
7. Mohammad, M., Hari, T.K., Yaakob, Z., Sharma, Y.C., Sopian, K.: Overview on the production of paraffin based-biofuels via catalytic hydrodeoxygenation. Renew. Sust. Energ. Rev. **22**, 121–132 (2013)
8. Thomas, R., Van Oers, E.M., De Beer, V.H.J., Medema, J., Moulijn, J.A.: Characterization of γ-alumina-supported Molybdenum oxide and tungsten oxide; reducibility of the oxidic state versus hydrodesulfurization activity of the sulfided state. J. Catal. **76**, 241–253 (1982)
9. Ayodele, O.B., Togunwa, O.S., Abbas, H.F., Daud, W.M.W.: Preparation and characterization of alumina supported nickel-oxalate catalyst for the hydrodeoxygenation of oleic acid into normal and iso-octadecane biofuel Energ. Convers. Management. **88**, 1104–1110 (2014)
10. Bui, P., Antonio, J., Oyama, S.T., Takagaki, A., Molina, A.I., Zhao, H., Li, D., Castellon, E.R., Lopez, A.J.: Studies of the synthesis of transition metal phosphides and their activity in the hydrodeoxygenation of a biofuel model compound. J. Catal. **294**, 184–198 (2012)
11. Jenistova, K., Hachemi, I., Arvela, P.M., Kumar, N., Peurla, M., Capek, L., Warna, J., Murzin, D.Y.: Hydrodeoxygenation of stearic acid and tall oil fatty acids over Ni-alumina catalysts: influence of reaction parameters and kinetic modelling. Chem. Eng. J. **316**, 401–409 (2017)
12. Ayodele, O.B., Farouk, H.U., Mohammed, J., Uemura, Y., Daud, W.M.A.W.: Hydrodeoxygenation of oleic acid into n- and iso-paraffin biofuel using zeolite supported fluoro-oxalate modified molybdenum catalyst: kinetics study. J. Taiwan Inst. Chem. E. **50**, 142–152 (2015)
13. Imai, H., Kimura, T., Terasaka, K., Li, X., Sakashita, K., Asaoka, S., AlKhattaf, S.S.: Hydroconversion of fatty acid derivative over supported Ni-Mo catalysts under low hydrogen pressure. Catal. Today **303**, 185–190 (2018)
14. Coumans, A.E., Hensen, E.J.M.: A real support effect on the hydrodeoxygenation of methyl oleate by sulfide NiMo catalysts. Catal Today. **298**, 181–189 (2017)
15. Kordouli, E., Sygellou, L., Kordulis, C., Bourikas, K., Lycourghiotis, A.: Probing the synergistic ratio of the NiMo/γ-Al_2O_3 reduced catalysts for the transformation of natural triglycerides into green diesel. Appl. Catal. B. **209**, 12–22 (2017)
16. Pattanaik, B.P., Misra, R.D.: Effect of reaction pathway and operating parameters on the deoxygenation of vegetable oils to produce diesel range hydrocarbon fuels: a review. Renew. Sust. Energ. Rev. **73**, 545–557 (2017)
17. Sapunov, V.N., Stepacheva, A.A., Sulman, E.M., Wärnåc, J., Arvela, P.M., Stein, B.D., Murzin, D.Y., Matveeva, V.G.: Stearic acid hydrodeoxygenation over Pd nanoparticles embedded in mesoporous hypercrosslinked polystyrene. Ind. Eng. Chem. **46**, 426–435 (2017)
18. Zhou, L., Lawal, A.: Kinetic study of hydrodeoxygenation of palmitic acid as a model compound for microalgae oil over Pt/γ-Al_2O_3. Appl. Catal. A Gen. **532**, 40–49 (2017)
19. Kandel, K., Anderegg, J.W., Nelson, N.C., Chaudhary, U., Slowing, I.I.: Supported iron nanoparticles for the hydrodeoxygenation of microalgal oil to green diesel. J. Catal. **314**, 142–148 (2014)
20. Tiwari, R., Rana, B.S., Kumar, Ro, Verma, D., Kumar, Ra, Joshi, R.K., Garg, M.O., Sinha, A.K.: Hydrotreating and hydrocracking catalysts for processing of waste soya-oil and refinery-oil mixtures. Catal. Commun. **12**, 559–562 (2011)
21. Yang, Y., Wang, Q., Zhang, X., Wang, L., Li, G.: Hydrotreating and hydrocracking catalysts for processing of waste soya-oil and refinery-oil mixtures. Fuel. Process. Technol. **116**, 165–174 (2013)
22. Zhou, Z., Zhang, W., Sun, D., Zhu, L., Jiang, J.: Renewable biofuel production from hydrocracking of soybean biodiesel with a commercial petroleum Ni-W catalyst. Int. J. Green Energy **13**, 1185–1192 (2016)
23. Kumar, R., Rana, B.S., Tiwari, R., Verma, D., Kumar, R., Joshi, R.K., Garg, M.O., Sinha, A.K.: Hydroprocessing of jatropha oil and its mixtures with gas oil. Green Chem. **12**, 2232–2239 (2010)
24. Hollak, S.A.W., Gosselink, R.W., Van Es, D.S., Bitter, J.H.: Comparison of tungsten and molybdenum carbide catalysts for the hydrodeoxygenation of oleic acid. ACS Catal. **3**, 2837–2844 (2013)
25. Hancsók, J., Kasza, T., Kovács, S., Solymosi, P., Holló, A.: Production of bioparaffins by the catalytic hydrogenation of natural triglycerides. J. Clean. Prod. **34**, 76–81 (2012)
26. Wachs, I.E., Kim, T., Ross, E.I.: Catalysis science of the solid acidity of model supported tungsten oxide catalysts. Catal. Today **116**, 162–168 (2006)
27. Oyama, S.T., Wang, X., Requejo, F.G., Sato, T., Yoshimura, Y.: Hydrodesulfurization of petroleum feedstocks with a new type of nonsulfide hydrotreating catalyst. J. Catal. **209**, 1–5 (2002)
28. Echeandia, S., Aria, P.L., Barrio, V.L., Pawelec, B., Fierro, J.L.G.: Synergy effect in the HDO of phenol over Ni–W catalysts supported on active carbon: effect of tungsten precursors. Appl. Catal. B. **101**, 1–12 (2010)
29. Sankaranarayanan, T.M., Berenguer, A., Ochoa-Hernández, C., Morenoa, I., Jana, P., Coronado, J.M., Serrano, D.P., Pizarro, P.: Hydrodeoxygenation of anisole as bio-oil model compound over supported Ni and Co catalysts: effect of metal and support properties. Catal. Today **243**, 163–172 (2015)
30. Rodrı´guez-Castello´, E., Jime´nez-Lo´pez, A., Eliche-Quesad, D.: Nickel and cobalt promoted tungsten and molybdenum sulfide mesoporous catalysts for hydrodesulfurization. Fuel **87**, 1195–1206 (2008)
31. Mendoza-Nieto, J.A., Vera-Vallejo, O., Escobar-Alarcón, L., SolísCasados, D., Klimov, T.: Development of new trimetallic NiMoW catalysts supported on SBA-15 for deep hydrodesulfurization. Fuel **110**, 268–277 (2013)
32. Janampelli, S., Darbha, S.: Selective and reusable Pt-WO_x/Al_2O_3 catalyst for deoxygenation of fatty acids and their esters to diesel-range hydrocarbons. Catal. Today **309**, 219–226 (2018)
33. Ng, K.T., Hercules, D.M.: Studies of nickel-tungsten-alumina catalysts by x-ray photoelectron spectroscopy. J. Phys. Chem. **80**, 2094–2102 (1976)
34. Hong, Y.K., Lee, D.W., Eom, H.J., Lee, K.Y.: The catalytic activity of *Sulfided* Ni/W/TiO_2 (anatase) for the hydrodeoxygenation of Guaiacol. J. Mol. Catal. A Chem. **392**, 241–246 (2014)
35. Nikulshin, P.A., Salnikov, V.A., Varakin, A.N., Kogan, V.M.: The use of CoMoS catalysts supported on carbon-coated alumina for hydrodeoxygenation of guaiacol and oleic acid. Catal. Today **271**, 45–55 (2016)